Synthesis, structural and spectral properties of Au complexes: Luminescence properties and their non-covalent DNA binding studies

ARTICLE *in* APPLIED ORGANOMETALLIC CHEMISTRY · AUGUST 2013

Impact Factor: 2.25 · DOI: 10.1002/aoc.3035

7 AUTHORS, INCLUDING:

Carlos Alberto Huerta Aguilar
Universidad Nacional Autónoma de México
14 PUBLICATIONS **7** CITATIONS
SEE PROFILE

Ignacio Camacho-Arroyo
Universidad Nacional Autónoma de México
139 PUBLICATIONS **1,935** CITATIONS
SEE PROFILE

Aliesha González-Arenas
Universidad Nacional Autónoma de México
36 PUBLICATIONS **462** CITATIONS
SEE PROFILE

Jayanthi Narayanan
Universidad Politécnica del Valle de México
19 PUBLICATIONS **85** CITATIONS
SEE PROFILE

Full Paper

Applied Organometallic Chemistry

Received: 16 May 2013 Revised: 18 June 2013 Accepted: 23 June 2013 Published online in Wiley Online Library

(wileyonlinelibrary.com) DOI 10.1002/aoc.3035

Synthesis, structural and spectral properties of Au complexes: luminescence properties and their non-covalent DNA binding studies

Carlos Huerta-Aguilar[a], Jose M. Talamantes Gómez[a], Pandiyan Thangarasu[a]*, Ignacio Camacho-Arroyo[a], Aliesha González-Arenas[a], Jayanthi Narayanan[b] and Rajendra Srivastava[c]*

Gold complexes of 1,3- bis-pyridylimidazolium chloride (L^1), 1,3-bis-[2,6-diisopropylphenyl]imidazolium chloride (L^2) and 1,3-bis-[benzyl]benzimidazolium chloride (L^3) were synthesized and characterized by analytical methods. For the complexes, electronic spectral results show that there is a marked difference in the band feature observed in the spectra, ascribed to the greater relativistic effect of gold. In fluorescence studies, the complexes develop emission bands in the visible region (400–600 nm) after excitation at around 350 nm. Au complex–DNA binding was studied, and it was observed that genomic DNA isolated from the U373-GB cell line was fragmented and in some cases degraded by the Au complexes. Furthermore, the intensity of the DNA band increased when concentration of the metal complex was augmented. This study shows that the DNA cleavage is mediated by the Au complex. Copyright © 2013 John Wiley & Sons, Ltd.

Supporting information may be found in the online version of this article.

Keywords: gold complexes; DNA binding; DFT

Introduction

Development of metal-based drugs has prospered consistently since the discovery of cisplatin, *cis*-[$Pt(NH_3)_2Cl_2$], as basic chemotherapeutics [1,2] because the adduct formation of cisplatin with DNA triggers apoptosis (therapeutic effect).[3] Along with cisplatin, other platinum(II) drugs, such as carboplatin and oxaliplatin, also continue to play a central role in the treatment of cancer and are used in chemotherapeutic regimes of around half of all cancer patients.[4] Despite tremendous efforts to improve therapy and recent advances, the spectrum of available effective drugs is comparatively limited and there is a considerable need for the development of new drugs and treatment alternatives. Although cisplatin is one of the most active anticancer drugs and is curative in some tumor types, it causes a severe problem in clinical treatment because of its side effects and acquired cellular resistance.[5,6] These drawbacks motivate the search for alternative chemotherapeutic strategies that can eliminate tumors without side effects and this is now a challenging task, requiring an understanding of the mechanisms by which tumors and cells distribute and process metal-based drugs. For clinical use, anticancer agents have to be proved by showing that they damage DNA or block DNA synthesis. Thus the development of new anticancer drugs based on non-platinum metal complexes is growing rapidly so as to develop new agents with a mode of action and clinical profile different from the established platinum metallodrugs.[7–9] Among the new non-platinum drugs, gold species have gained particular attention because of their generally strong tumor cell growth-inhibiting effects and the observation that many of these compounds inhibit the enzyme thioredoxin reductase (TrxR), a key enzyme for cell growth and survival, with high potency and specificity.[10]

In the literature, gold complexes have been studied for potential antitumor properties,[11–15] and it was shown that complexes of the type [(R_3P)Au(thiolate)] exhibit antitumor properties;[16–18] furthermore, gold(I) phosphane derivatives or gold(I) complexes of bisphosphanes have also shown significant activity in murine tumor.[16,19] In addition, although gold(I) complexes like [(dppe)$_2$Au]$^+$ (dppe = 1,2-bis-(diphenylphosphino)ethane) exhibit promising cytotoxicity in preclinical studies,[20–22] they produce other severe adverse effects (cardiac, hepatic and vascular toxicity).[23,24] Therefore, considerable effort has now been focused on the development of new anticancer drugs based on Au complexes of different ligands. In this work we studied the structural, spectral and DNA binding properties of a series of gold complexes with 1,3-bis-pyridylimidazolium chloride (L^1), 1,3-bis-[2,6-diisopropylphenyl]imidazolium chloride (L^2) and 1,3-bis-[benzyl] benzimidazolium chloride (L^3) (Fig. 1). The ligands are used to

* *Correspondence to: Pandiyan Thangarasu, Facultad de Química, Universidad Nacional Autónoma de México (UNAM), Ciudad Universitaria, Coyoacán 04510, México DF, México. E-mail: pandiyan@unam.mx;*

Rajendra Srivastava, Department of Chemistry, Indian Institute of Technology Ropar, Rupnagar, Panjab 140001, India. E-mail: rsrivastava@ku.edu

a *Facultad de Química, Universidad Nacional Autónoma de México (UNAM), Ciudad Universitaria, Coyoacán 04510, México DF, México*

b *Ingeniería en Nanotecnología, Universidad Politécnica del Valle de México, CP 54910, Tultitlán, Estado de México*

c *Department of Chemistry, Indian Institute of Technology Ropar, Rupnagar, Panjab 140001, India*

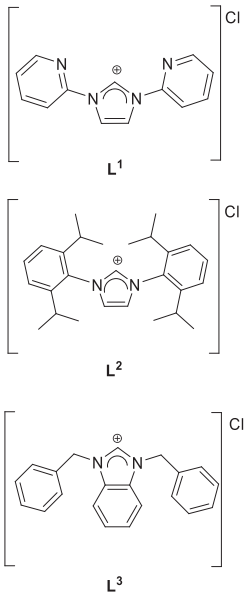

Figure 1. Structures of ligands: $\mathbf{L^1}$ = 1,3-bis(aminopyridyl-2-yl)imidazolium chloride; $\mathbf{L^2}$ = 1,3-bis-[2,6-diisopropylphenyl]imidazolium chloride; $\mathbf{L^3}$ = 1, 3-bis-[benzyl] benzimidazolium chloride.

tune the solubility and lipophilicity of the gold complexes, which, in turn, have a marked influence on their binding properties against the cancer cell lines. The structural and electronic parameters of the Au complexes were described by density functional theory (DFT).

Experimental/Computational Details

Physical Measurements

Elemental analyses for the compounds were carried out on a Fisons (Model EA 1108 CHNSO) element analyzer. ^{1}H NMR spectra were recorded for the compounds on a Varian Gemini (300 MHz) spectrometer using tetramethylsilane as an internal standard. A mass spectrometer (FAB-MS) (model Thermo-Electron) equipped with double focus sector was used to analyze the mass fragments of the compounds. For the complex, the electronic spectrum was measured in methanol by a PerkinElmer Lambda-25 double beam UV–visible/NIR spectrophotometer. A fluorescence spectrophotometer (Varian Eclipse) was employed to analyze the luminescence properties of the compounds.

Computational Procedure

The DFT calculations were performed by means of Gaussian-09 software[25] for 1,3-bis-pyridylimidazolium chloride ($\mathbf{L^1}$), 1,3-bis-[2,6-diisopropylphenyl]imidazolium chloride ($\mathbf{L^2}$) and 1,3-bis-[benzyl]benzimidazolium chloride ($\mathbf{L^3}$). For the ligands, calculations were carried out at B3LYP with base set 6-311G,[26,27] while for the complexes $[Au(\mathbf{L_2^1})]^+$, $[Au(\mathbf{L_2^2})]^+$ and $[Au(\mathbf{L_2^3})]^+$ B3LYP with unrestricted spin method LANL2DZ[28] was used. The exchange correlation was treated and the choice of this method was based on results obtained from the previous calculation used for C, N, Cl and H atoms. For Au^+, pseudo-potential was used. The structures of $\mathbf{L^1}$, $\mathbf{L^2}$ and $\mathbf{L^3}$ were fully optimized and the data were then used as the input for the optimization of gold complexes.

Materials

All commercially available reagents employed were: formaldehyde 99%, 2-aminopyridine, 2,6-diisopropylphenylamine, benzylamine, aqueous glyoxal, tetrahydrothiophene, $HAuCl_4.4H_2O$ (Aldrich); all solvents MeOH, EtOH, ethylic ether and CH_2Cl_2 (Baker) were utilized without any further purification.

Preparation of 1,3-bis(aminopyridyl-2-yl)imidazolium chloride ($\mathbf{L^1}$)

Ligand $\mathbf{L^1}$ was prepared following the reported procedure.[29] To a stirred solution of 2-aminopyridine (10.0 mmol) in MeOH (40.0 ml) was added aqueous glyoxal (5.0 mmol) and paraformaldehyde (5.0 mmol), followed by dropwise addition of HCl (5.0 mmol). The resulting mixture was refluxed for 36 h with stirring and then cooled to room temperature. The brown oily compound was obtained by evaporating the solvent in a rotary evaporator. The compound was recrystallized by dissolving with a minimum amount of methanol and ether solvent (yield 53.0%). Elemental analysis for $C_{13}H_{11}N_4Cl$. Calcd: C, 60.34; H 4.25; N 21.66. Found: C 60.45; H 4.29; N 21.76. ^{1}H NMR (300 MHz, CD_3OD) δ (ppm): 8.73 (s, 1H, —N—CH=N—, imidazole H); 8.21 (d, 2H, —C=N—**CH**=CH—, pyridyl H); 7.82 (d-d, 2H, —N=C—CH=**CH**—CH, pyridyl H); 7.32 (d, 2H, —N—CH=CH—N, imidazole H); 6.86 (t, 2H, —N=C—CH=CH—**CH**=CH, pyridyl H); 6.89 (d, 2H, —N=C—**CH**=CH—, pyridyl H).

1,3-Bis(2,6-diisopropylphenyl)imidazolium chloride ($\mathbf{L^2}$)

Synthesis and structural characterization of gold(I)[30] and silver (I)[31] complexes using the ligand $\mathbf{L^2}$, which was then prepared by the published method;[32,33] although these complexes were synthesized from NHC (*N*-heterocyclic carbene) rather than the imidazolium chloride, for the present work ligand $\mathbf{L^2}$ was prepared following the reported procedure.[34] A mixture of glyoxal (5.0 mmol) and formaldehyde (5.0 mmol) was added to a solution of 2,6-diisopropylphenilamine (10.0 mmol) and methanol (40.0 ml), followed by dropwise addition of HCl (5.0 mmol). The reaction mixture was refluxed for 36 h and then cooled to room temperature. An oily compound was obtained by evaporating the solvent in a rotary evaporator. The compound was recrystallized by dissolving in a minimum amount of methanol and ether solvent (yield 84.6%). Elemental analysis for $C_{27}H_{37}N_2Cl$. Calcd: C, 76.32; H, 8.71; N, 6.59. Found: C, 75.30; H, 8.49; N, 6.79. ^{1}H NMR (300 MHz, CD_3OD) δ (ppm): 10.07 (s, 1H, —N—CH=N—, imidazole H); 8.39 (d, 2H, N—CH=CH—N, imidazole H); 7.69 (t, 2H, —C=C—CH=**CH**—CH, phenyl H); 7.52 (d, 8H, —C=C—**CH**=CH—, phenyl H); 2.84 (m, 4H, —CH—$(CH_3)_2$, isopropyl H); 1.29 (d, 24H, —CH_3—CH—, isopropyl H).

1,3-Bis(benzyl)benzimidazolium chloride ($\mathbf{L^3}$)

Even though a different synthesis of ligand $\mathbf{L^3}$ was reported in the literature,[35] the compound was prepared as cited for $\mathbf{L^1}$. To a stirred solution of benzylamine (10.0 mmol) in MeOH (40.0 ml), aqueous glyoxal (5.0 mmol) and paraformaldehyde (5.0 mmol) were added, followed by the dropwise addition of HCl (5.0 mmol). This mixture was refluxed for 36 h under continuous stirring and then left to cool to room temperature. The yellow oily compound was obtained after the evaporation of solvent in a rotary evaporator. Recrystallization was achieved by dissolving the product with a minimum amount of methanol and ether (yield 64.0%).

Elemental analysis for $C_{21}H_{19}N_2Cl$. Calcd: C, 75.33; H, 5.72; N, 8.37. Found: C, 75.84; H, 5.96; N, 8.12; ^{1}H NMR (300 MHz CD_3OD) 8.08 (s, 1H, —N—CH=N—, imidazole H); 7.70 (d, 2H, —C—C**H**=CH, benzimidazole H); 7.26 (m, 2H, C—CH—C**H**=CH, benzimidazole H); 7.14–7.18 (m, 4H, CH—CH=CH, phenyl H); 7.06 (m, 6H, C=C—C**H**=CH, phenyl H); 4.99 (s, 4H, N—CH_2—C(phenyl)).

Synthesis of Au(I) Complexes

Preparation of chloro(tetrahydrothiophene)gold(I) [Au(tht)]Cl

[Au(tht)]Cl was prepared by following the reported procedure.[36] To a solution of $HAuCl_4$ (15.0 mmol) dissolved in solvent mixture (water:ethanol, 1:5), tetrahydrothiophene (31.75 mmol) was added slowly with stirring in dark conditions. In the initial stage of the reaction, a yellow-colored precipitate of $AuCl_3(SC_4H_8)$ was formed and it then changed to colorless product after the addition of tetrahydronthiophene was completed. The resulting mixture was stirred for 30 min at room temperature. The colorless product obtained was filtered, washed with ethanol (30 ml) and dried under vacuum. Yield 92.4%. The analytical and spectral data of the product were in good agreement with the reported values.

Preparation of gold complexes ([Au($\mathbf{L^1}_2$)]Cl.3EtOH, [Au($\mathbf{L^2}_2$)]Cl.2H_2O and [Au(L^3_2)]Cl.H_2O

The preparation of gold complexes was made through a modification of techniques previously reported.[29,37–39] Gold(I) complexes were prepared by the reaction of imidazole/benzimidazole ring-based ligands with [Au(tht)]Cl in CH_2Cl_2.

([Au($\mathbf{L^1}_2$)]Cl.3EtOH. To a solution of [Au(tht)]Cl (0.75 mmol) in CH_2Cl_2 (10.0 ml), a solution of ligand ($\mathbf{L^1}$, 1.5 mmol) in CH_2Cl_2 (20.0 ml) was added slowly under stirring. The resulting solution was stirred for 25 min at 308 K in the absence of light and the resulting oily product was obtained after evaporation; the product was recrystallized with a mixture of acetonitrile–ethanol and finally washed with ether. Pale-yellow solid; yield 76.4%. Anal.

Table 1. Optimized geometrical structural data of ligands and the complexes

	B3LYP/6-31G**			B3LYP/LANL2DZ		
	$\mathbf{L^1}$	$\mathbf{L^2}$	$\mathbf{L^3}$	$[Au\mathbf{L^1}_2]^+$	$[Au\mathbf{L^2}_2]^+$	$[Au\mathbf{L^3}_2]^+$
Bond distance (Å)						
C1—N1	1.357	1.354	1.352	1.378	1.374	1.374
C1—N2	1.357	1.353	1.352	1.381	1.338	1.374
N1—C2	1.406	1.401	1.414	1.400	1.404	1.412
N2—C3	1.406	1.401	1.414	1.399	1.344	1.412
C2—C3	1.371	1.376	1.418	1.375	1.352	1.412
N1—C4	1.451	1.467	1.491	1.447	1.611	1.478
N2—C4′	1.451	1.465	1.491	1.445	1.436	1.478
N3—C4	1.342	—	—	1.346	—	—
N3′—C4′	1.342	—	—	1.345	—	—
C4—C5	—	1.419	1.522	—	1.407	1.524
C4—C6	—	1.422	—	—	1.452	—
C4′—C5′	—	1.418	1.522	—	1.409	1.524
C4′—C6′	—	1.418	—	—	1.370	—
Au1—C1	—	—	—	2.054	1.955	2.056
Au1—C1′	—	—	—	2.069	2.086	2.056
Angle (°)						
N1—C1—N2	108.17	108.90	110.67	105.18	107.03	106.66
C1—N1—C4	127.65	125.64	125.39	127.67	136.03	125.15
C1—N2—C4′	127.65	125.62	125.39	120.71	126.43	125.15
C1—N2—C3	108.81	108.44	108.11	110.62	108.40	110.38
C1—N1—C2	108.81	108.32	108.11	110.61	102.19	110.38
C4—N1—C2	123.53	125.79	126.48	121.69	120.65	124.43
N1—C4—N3	113.54	—	—	122.25	—	—
C4′—N2—C3	123.53	—	—	128.64	—	—
N1—C2—C3	107.10	107.23	106.55	107.24	107.20	106.28
N2—C3—C2	107.10	107.09	106.55	106.32	106.91	106.28
N3—C4—N1	113.54	—	—	113.64	—	—
N3′—C4′—N2	113.54	—	—	114.57	—	—
C5—C4—C6	—	123.35	—	—	116.70	—
C5′—C4′—C6′	—	123.65	—	—	120.25	—
N1—C4—C5	—	—	113.50	—	—	113.98
N2—C4′—C5′	—	—	113.50	—	—	113.97
C1—Au1—C1′	—	—	—	177.27	169.61	179.82
N1—C1—Au1	—	—	—	138.34	135.86	126.78
N2—C1—Au1	—	—	—	116.36	116.98	126.55

Calcd for $[C_{26}H_{20}N_8Au]Cl.3CH_3CH_2OH$: C, 47.15; H, 4.70; N, 13.75. Found: C, 47.90; H, 4.35; N, 14.96; IR (KBr, cm^{-1}): 3300 (O—H), 3061–2866 (C—H, py), 1715 (C=N, py), 1468–1434 (C=C; C=N, im), 768 (C—H). ^{1}H NMR (300 MHz, acetone-d_6) δ (ppm) = 8.36–8.40 (d, 4H, —N=C**H**—CH—, pyridyl H); 8.11–8.22 (d, d, 4H, —N=C—CH=C**H**—CH—, pyridyl H); 7.84 (d, 4H, —N—CH=CH—N— imidazole H); 7.22 (d, d, 4H, —CH—C**H**—CH—N=C—, pyridyl H); 6.88 (d, 4H, —N=C—C**H**=CH—, pyridyl H). ^{13}C NMR (300 MHz, $CDCl_3$) δ (ppm) = 150.1, 142.4, 115.2, 108.9 (20C, pyridyl C); 129.9 (2C, —N—C=N— , imidazole C); 115.2 (4C, —N—CH=CH—N—, imidazole C); FAB-MS (*m/z* %): 815 $[M^+, C_{32}H_{38}AuClN_8O_3]^+$, 663 (6.0%) $[C_{26}H_{26}AuN_8O]^+$, 309 (12.0 %) $[C_4H_8AuN_4]^+$, 153 (100%) $[C_7H_{13}N_4]^+$, 136 (90.0 %) $[C_6H_9N_4]^+$, 107 (54.0%) $[C_6H_7N_2]^+$, 57 (66.0 %) $[C_3H_7N]^+$.

*Au(**L**$^2_2$)]Cl.2H$_2$O.* To a stirred solution of [Au(tht)]Cl (0.75 mmol) in CH_2Cl_2 (10.0 ml), the solution of ligand **L**^{2} (1.5 mmol) in 20.0 ml CH_2Cl_2 was added dropwise in the absence of light. The reaction was heated to 308 K and left for 30 min to react; the resulting yellow precipitate was filtered and finally recrystallized in a mixture of acetonitrile–ethanol and washed with ether. Colorless solid; yield 89.3%; Anal. Calcd for $[C_{54}H_{72}N_4Au]Cl.2H_2O$: C, 62.03; H, 7.33; N, 5.36. Found: C, 60.95; H, 6.41; N, 5.23; IR (KBr, cm^{-1}): 3281 (O—H), 2967 (C—H, bz), 2931 (C—H), 1544 (C=C; C=N, im). ^{1}H NMR (300 MHz, acetone-d_6) δ (ppm) = 8.24 (d, 4H, N—CH=CH—N, imidazole H,); 7.66–7.62 (t, 4H, —C=C—CH=C**H**—CH—, phenyl H); 7.51 (d, 8H, —C=C—C**H**=CH— phenyl H); 2.46 (m, 8H, —C**H** $(CH_3)_2$, isopropyl H); 1.33 (d, 48H, —CH (**CH$_3$**)$_2$, isopropyl). ^{13}C NMR (300 MHz, $CDCl_3$) δ (ppm) = 149.9, 136.8, 135.1, 129.4 (24C, phenyl C); 144.5 (2C, —N—C=N—, imidazole C); 131 (4C, —N—CH=CH—N—, imidazole C); FAB-MS (*m/z* %): 1042 $[M^{2+}, C_{54}H_{76}AuClN_4O_2]^{2+}$, 389 (100%) $[C_{27}H_{36}N_2]^+$, 186 (10.0%) $[C_{12}H_{14}N_2]^+$, 91 (3.0%) $[C_6H_5N]^+$.

[Au(L$^3_2$)]Cl.H$_2$O. To a stirred solution of [Au(tht)]Cl (0.75 mmol) in CH_2Cl_2 (10.0 ml), a solution of **L**^{3} (1.5 mmol) in CH_2Cl_2 (20.0 ml) was added dropwise under continuous stirring. The resulting solution was left to react for 30 min at 308 K and in the absence of light. The resulting pale-brown oil was obtained by evaporation of solvents and recrystallized in acetonitrile–ethanol. Finally, the product was washed with ether and the precipitate was filtered. Pale solid; yield 85.5%. Anal. Calcd for $C_{42}H_{38}N_4Au]Cl.H_2O$: C, 59.54; H, 4.52; N, 6.61. Found: C, 60.95; H, 4.41; N, 6.23; IR (KBr, cm^{-1}): 3650 (O—H), 3086–3023 (C—H), 1522 (C=C; C=N, im), 728 (C—H). ^{1}H NMR (300 MHz, acetone-d_6) δ (ppm) = 7.66 (d, 4H, —C—C**H**=CH—, benzimidazol H); 7.46–7.52 (t, 4H, —C—CH=C**H**—CH— , benzimidazol H); 7.33 (d, d, 8H, —C=CH—C**H**=CH—, phenyl H); 7.21–7.31 (m, 12H, —C=C**H**—CH— phenyl H); 5.55 (s, 8H, —N—CH_2—C(phenyl)). ^{13}C NMR (300 MHz, $CDCl_3$) δ (ppm) = 132.8 (2C, N—C=N, imidazole C); 132.0, 119.3, 111.2 (12C, benzimidazole C); 129.6, 127.8, 125.8, 125.0 (24C, phenyl C); 50.2 (4C, —N—CH_2—C (phenyl)); FAB-MS (*m/z* %): 846 $[M^+, C_{42}H_{37}N_4AuCl].H_2O^+$, 663 (38.0%) $[C_{20}H_{30}N_2]^+$, 613 (62.0%) $[C_{15}H_{21}N_2]^+$, 299 (25.0%) $[C_9H_{18}N_2]^+$, 154 (100%) $[C_9H_{15}N]^+$, 136 (88.0%) $[C_9H_{15}N]^+$, 91 (54.0%) $[C_6H_5]^+$.

Note: Although we tried to grow single crystals of the complexes for X-ray structure analysis under different conditions in different solvents, we were unsuccessful, in that the crystals obtained were not suitable for structural analysis.

Cell culture. The U373-GB cell line derived from human astrocytomas grade III (ATCC, Manassas, VA, USA) was employed to analyze the binding properties of the complexes. The culture experiments were performed as described elsewhere.[40,41] The cells (300 000) were incubated on six tissue culture plates (10 cm dishes) and maintained in Dulbecco's modified Eagle's medium (DMEM), then supplemented with fetal bovine serum (10%), pyruvate (1.0 mM), glutamine (2.0 mM) and non-essential amino acids (0.1 mM) (GIBCO, NY, UDA). The experiment was carried out at 37 °C for 24 h under an atmosphere of 95% air and 5% CO_2. The cells were treated with each complex (1 μM) at different concentrations (500 nM to 10.0 μM). DMSO (10%) in water was used as vehicle. After treatment, the cells were lysed and processed with Spin Micro DNA Kit (Invisorb) to isolate and purify the DNA.

DNA binding studies with Au complex. The interaction of Au complexes with genomic DNA isolated from the U373-GB cell line (1.0 μg) was studied and analyzed on 1.0% agarose gel and stained with gel red (Biotium, CA, USA); in the experiment, a loading buffer, i.e. a mixture of bromophenol blue (25%), xylene cyanol (0.25%) and glycerol (3.0 ul, 30%) was added.

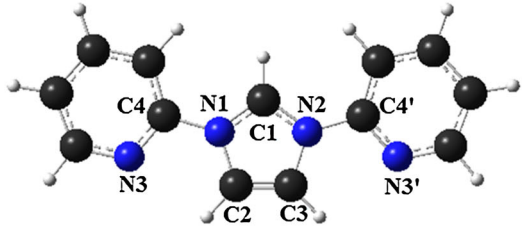

L^1

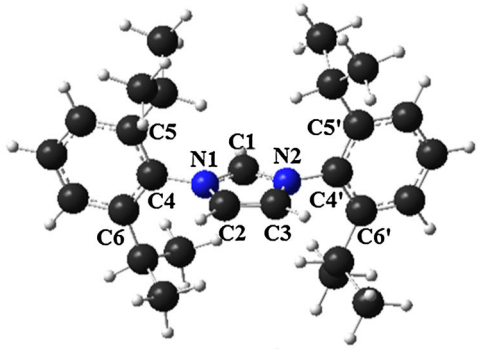

L^2

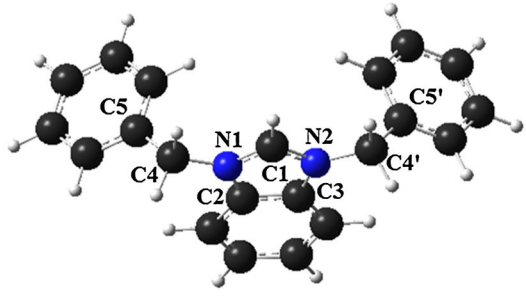

L^3

Figure 2. Optimized structures of ligands: **L**^{1} = 1,3-bis(aminopyridyl-2-yl) imidazolium chloride; **L**^{2} = 1,3-bis-[2,6-diisopropylphenyl]imidazolium chloride; **L**^{3} = 1,3-bis-[benzyl] benzimidazolium chloride.

Electrophoresis was performed at 70 V for 2.0 hours in Tris–acetate–ethylenediaminetetraacetic acid (EDTA) buffer (40 mM Tris base, 20 mM acetic acid, 1.0 mM EDTA). The image was captured under a UV transilluminator using a Canon SD1400IS camera.

Results and Discussion

Geometrical Analysis of Ligand and Gold Complexes

For 1,3-bis-pyridylimidazolium chloride ($\mathbf{L^1}$), 1,3-bis-[2,6-diisopropylphenyl]imidazolium chloride ($\mathbf{L^2}$) and 1,3-bis-[benzyl] benzimidazolium chloride ($\mathbf{L^3}$), the ground state geometrical data (Table 1 and Fig. 2) show that for all the ligand structures the bond distance of C—N was around 1.34–1.45 A. The charge distribution over the ligands, particularly on imidazolium centers, was analyzed (Table 2). The results indicate that there is present an excess electron density over the imidazolium ring that can facilitate bond formation with the metal. Besides, the hardness of the ligand, determined by (LUMO-HOMO)/2),[42,43] shows that the ligand can coordinate efficiently with Au^+. In the molecular orbital analysis, since the energy difference between HOMO (−6.14 eV), and HOMO-1 (−6.28 eV) is very small, both orbitals can be involved cooperatively in bonding with the metal (Table 3). Thus, in the ligand, the orbitals HOMO and HOMO-1 are localized over N1—C1=N3 of the imidazole ring (see supporting information, Fig. S7), which favors the formation of bonds with Au(I). This is consistent with the Mulliken charge densities.

The structures of $[Au(L^1_2)]^+$, $[Au(L^2_2)]^+$ and $[Au(L^3_2)]^+$ were optimized and the results show (Fig. 3) that two ligands $\mathbf{L^1}$ are coordinated with Au(I) ion in such a way that the metal ion exhibits a linear geometry. In the structure, Au(I) is bonded with two C_{carb} (imidazolium ring), forming a linear structure consisting of C(1), C′(1′) atoms and their distances with the metal ion are 2.054, 2.069 Å ($[Au\mathbf{L^1}_2]^+$); 1.955, 2.086 Å $[Au\mathbf{L^2}_2]^+$; 2.056, 2.056 Å ($[Au\mathbf{L^3}_2]^+$) (Table 2); the a bond lengths calculated are agreed with the published bond lengths.[30,44] The resulting bond angles for *trans* bonded atoms around the metal center are: 177.27° for C(1)—Au(1)—C(1′) ($[Au\mathbf{L^1}_2]^+$); 169.61° for $[Au\mathbf{L^2}_2]^+$, 179.82° for $[Au\mathbf{L^3}_2]^+$, showing that the metal presents a distorted linear structure. This is consistent with reported results that a two-coordinate gold(I) linear structure presents a twofold axis[30,45]. For the case of $[Au\mathbf{L^2}_2]^+$ and $[Au\mathbf{L^3}_2]^+$, a similar observation was found and the bond distance

Table 2. Charge density data of ligands and complexes

Mullikencharge	B3LYP/6-31G**			B3LYP/LANL2DZ		
	$\mathbf{L^1}$	$\mathbf{L^2}$	$\mathbf{L^3}$	$[Au\mathbf{L^1}_2]^+$	$[Au\mathbf{L^2}_2]^+$	$[Au\mathbf{L^3}_2]^+$
C1	−0.042	−0.109	−0.085	−0.159	−0.182	−0.235
C2	−0.143	−0.172	0.250	−0.152	−0.201	0.202
C3	−0.157	−0.190	0.250	−0.138	−0.205	0.204
C4	0.249	−0.057	−0.519	0.134	−0.001	−0.508
C5	—	0.525	0.504	—	−0.037	0.496
C6	—	0.529	—	—	−0.032	—
C4′	0.249	−0.113	−0.519	0.158	−0.014	−0.508
C5′	—	0.481	0.504	—	−0.037	0.496
C6′	—	0.519	—	—	−0.033	—
N1	−0.157	−0.236	−0.150	−0.207	−0.237	−0.198
N2	−0.157	−0.243	−0.150	−0.200	−0.266	−0.197
N3	−0.080	—	—	−0.034	—	—
N3′	−0.080	—	—	−0.041	—	—
Au1	—	—	—	0.877	1.637	0.677

Table 3. Molecular orbital energy data of ligands and data

Molecular Orbital (eV)	B3LYP/6-31G**			B3LYP/LANL2DZ		
	$\mathbf{L^1}$	$\mathbf{L^2}$	$\mathbf{L^3}$	$[AuL^1_2]^+$	$[AuL^2_2]^+$	$[AuL^3_2]^+$
LUMO + 3	−4.51686	−3.42846	−3.401	−6.802	−5.550	−2.802
LUMO + 2	−4.6257	−3.59172	−3.564	−7.237	−5.578	−2.938
LUMO + 1	−4.76175	−3.70056	−3.646	−7.482	−5.850	−3.809
LUMO	−5.82294	−4.65291	−5.197	−8.326	−6.965	−4.108
Delta	4.84338	4.92501	4.598	4.163	1.659	4.952
HOMO	−10.66632	−9.57792	−9.795	−12.489	−8.625	−9.060
Delta	0.2721	0.08163	0.027	0.680	0.707	0
HOMO-1	−10.93842	−9.65955	−9.822	−12.598	−9.333	−9.060
HOMO-2	−11.07447	−10.09491	−9.850	−12.652	−9.387	−9.088
HOMO-3	−11.26494	−10.17654	−9.850	−12.652	−9.795	−9.115
Hardness	2.421	2.462	2.299	2.272	0.83	2.476
Softness	0.412	0.406	0.434	0.440	1.204	0.403

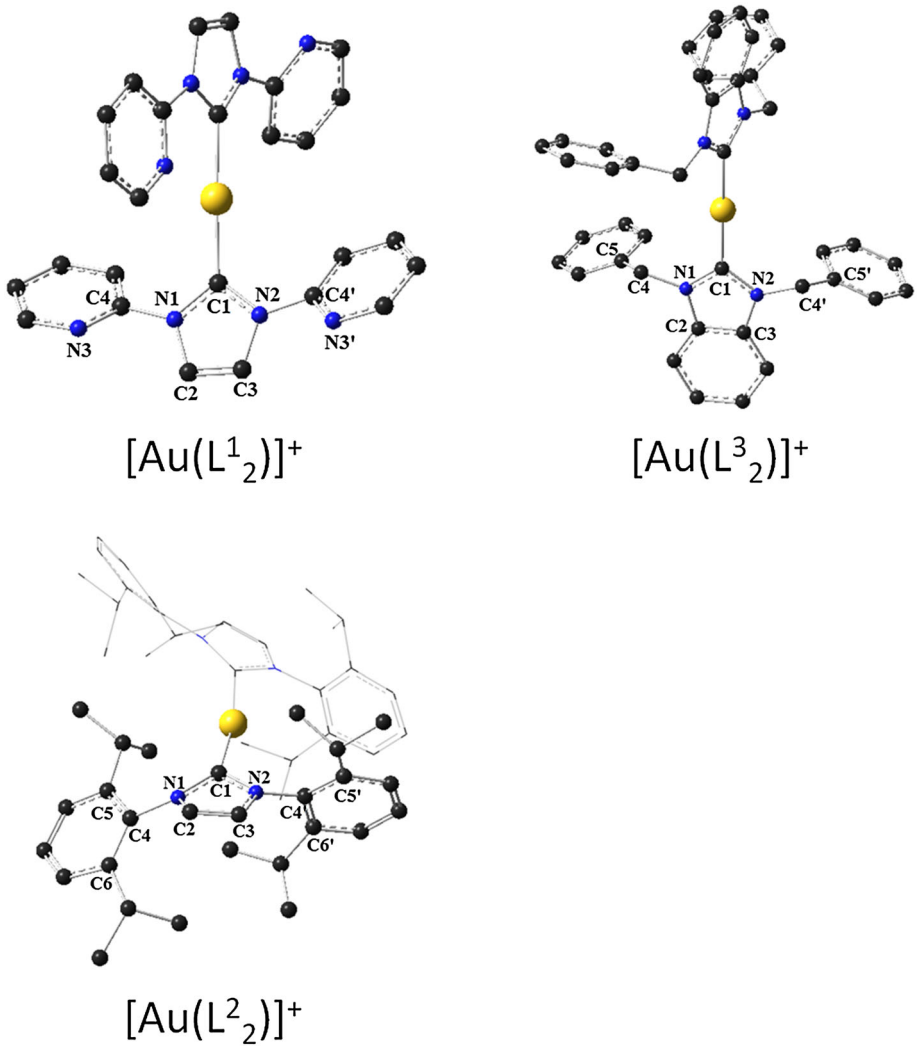

Figure 3. Structures of Au complexes.

and dihedral angles obtained for the complex are almost equal to the angles resulting for $[Au\mathbf{L}^{\mathbf{1}}{}_2]^+$. Among the ligands, the formation of complexes using $\mathbf{L}^{\mathbf{2}}$ with other metals (iron(II),[46] In(III),[47] Ga (II),[48] Cu(I),[49] Ge(II)[50]) is well established.

Furthermore, molecular orbital (MO) analysis (Fig. 4) establishes the formation of bonds through the mixing of the orbitals of Au(I) with those of the ligands; all low-lying HOMOs resulted from the overlap of metal and ligand orbitals. For instance, for $[Au\mathbf{L}^{\mathbf{1}}{}_2]^+$, the HOMO orbitals were obtained through combinations of d [Au(I)] and p orbitals of $\mathbf{L}^{\mathbf{1}}$; the orbitals (HOMO to HOMO-*X*; $X = 1–8$) (Fig. 4a, b, c) resulted from the mixing of the d orbital (metal) with π/p of the ligand, where $\mathbf{L}^{\mathbf{1}}$ contributes considerably to the π/p character of Au(II), the LUMO being derived through the combination of the π^* type [C(1), C(1′)] of ligands with d (Au^+). The LUMO is generated because of the d_z^2 (Au) mixture with the orbitals of atoms, thus confirming the existence of an Au(I)—C bond in the geometry. Moreover, the π-character of the ligand moiety presented in the complex was corroborated: the HOMO, and other low-lying orbitals (HOMO-*x* ($x = 1–8$) for $[Au\mathbf{L}]^+$ were observed. Similarly, the HOMO orbitals were obtained through the combinations of d [Au(I)] with the p orbitals of $\mathbf{L}^{\mathbf{2}}$ or $\mathbf{L}^{\mathbf{3}}$ for $[Au\mathbf{L}^{\mathbf{2}}{}_2]^+$ or $[Au\mathbf{L}^{\mathbf{3}}{}_2]^+$.

Electronic Absorption and Emission Spectra

The absorption spectra of the Au complexes recorded (Fig. 5 and Table 4) in MeOH and CH_2Cl_2 show that there are peaks in the high-energy region (192–216 nm); it was seen that all the compounds exhibit similar spectral features and the substituent groups present in the ligand produce negligible variation in the spectra. This is consistent with reports[51,52] that substituents hardly present a variation in the electronic spectra of Au complexes. However, a low-energy band appears at 392 nm for [Au ($\mathbf{L}^{\mathbf{1}}{}_2$)]Cl.3EtOH that is blue shifted to 282 nm for [Au($\mathbf{L}^{\mathbf{2}}{}_2$)]Cl.$2H_2O$ due to the inductive effect of *N*-substituted diisopropyl phenyl of the imidazolium ring ($\mathbf{L}^{\mathbf{2}}$). But the spectral behaviors of [Au ($\mathbf{L}^{\mathbf{2}}{}_2$)]Cl.$2H_2O$ and [Au($\mathbf{L}^{\mathbf{3}}{}_2$)]Cl.$H_2O$ were similar. This observation is consistent with reported results[30,31] that the alkyl-substituted NHCs are expected to be better donors than their aryl counterparts; however, the aryl-substituted NHC ligands are slightly more donating when they are bound to gold. The analysis of the Au—C (NHC) bond lengths as determined in structural studies[30] suggests that no major electronic differences between the various NHC ligands examined on coordination with the gold center. In the spectra, the intense bands have been assigned to

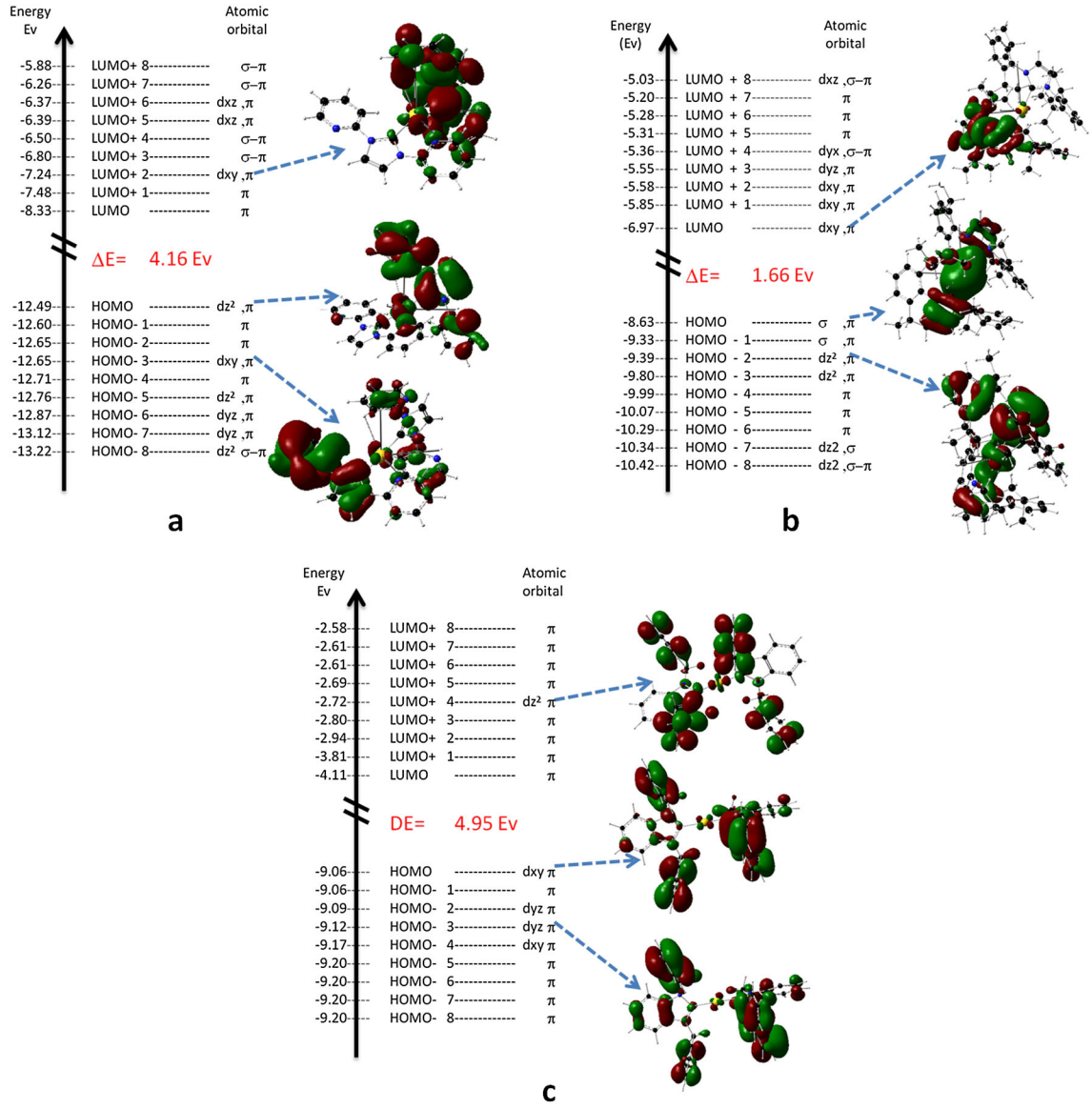

Figure 4. Molecular orbital energy diagram of Au complexes : (a) $[Au(\mathbf{L^1}_2)]^+$; (b) $[Au(\mathbf{L^2}_2)]^+$; (c) $[Au(\mathbf{L^3}_2)]^+$.

metal-to-ligand charge transfer (MLCT) from the filled gold d-orbitals.[53] Furthermore, it was noted that the intensity of the bands increased when the spectra were recorded at low temperature, due to the fact that interaction of the metal ion with the ligand became stronger at low temperature.

Additionally, for the complexes, luminescence properties were analyzed. The emission and excitation spectra of the complexes are shown in Fig. 6 and Table 5.

As seen in the electronic spectra, the low-energy emission band (428 nm) was observed for $[Au(\mathbf{L^1}_2)]Cl.3EtOH$; however, for $[Au(\mathbf{L^2}_2)]Cl.2H_2O$, the emission band appeared at higher energy (350 nm) than that for $[Au(\mathbf{L^1}_2)]Cl.3EtOH$ (428 nm) due to the structural inductive effect caused by the *N*-substituted diisopropyl phenyl of the imidazolium ring ($\mathbf{L^2}$), and for $[Au(\mathbf{L^3}_2)]Cl.H_2O$ there is no resonating current between the methylpyridyl group and the imidazolium ring, thus no significant change was seen in the spectra. The excitation profile (black line) shown was obtained while the emission was monitored in the fluorescence spectra (red and blue lines). It was seen that the emission spectra were dependent on the excitation wavelength because the change in the emission bands occurred when the excitation wavelength was changed. Although the excitation was carried out at different wavelengths, only at a specific excitation wavelength (see Table 5) was a considerable intense emission band observed. For example, for $([Au(L^1_2)]Cl.3EtOH$ (Fig. 6a), the excitation at 373 nm yields an intense emission band at 430 nm in the visible region; furthermore, the intensity of the emission band increased when the temperature of the compound solution was lowered from 25 to 2.0 °C, which is attributed to the increase of aurophilic interactions at the low temperature. For the fluorescence spectra, the excitation maximum was present at lower energies than the MLCT absorption band. The differences in the excitation profiles and the absorption spectra of these complexes reinforce the notion that the luminescence arises from the unique intermolecular interactions present in solution. Although the UV–visible spectra of the complexes are nearly identical, the luminescent features (λ max excitation and λ max emission) of each compound exhibit different behaviors at different temperatures. The aurophilic attractions in the compounds allow overlap of the occupied gold 5d orbitals

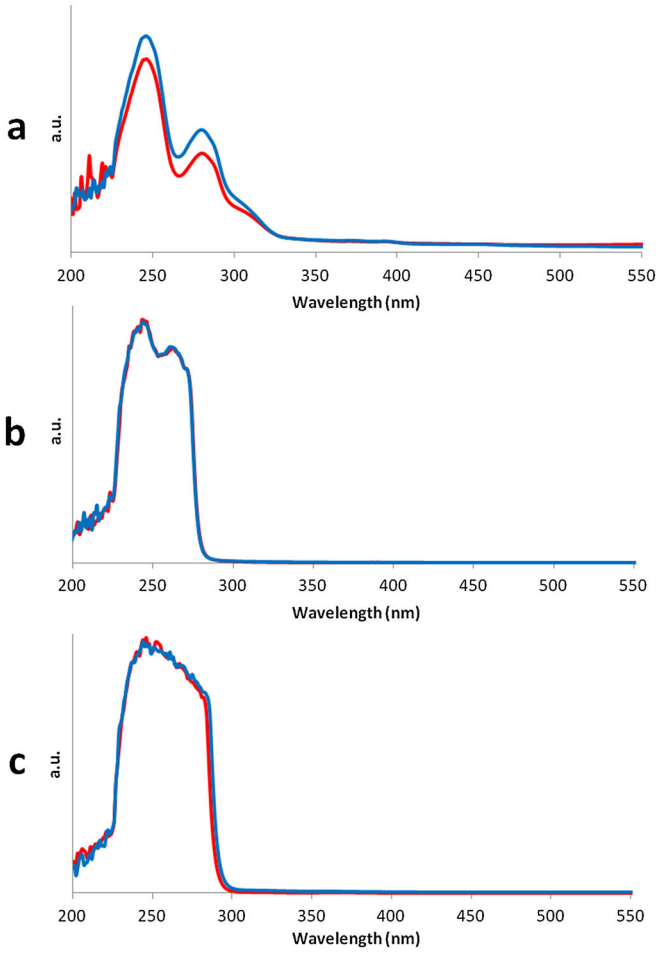

Figure 5. UV–visible absorption spectra (red: absorption at 20 °C; blue: absorption at 2 °C): (a) [Au($\mathbf{L^1}_2$)]Cl.3EtOH ; (b) [Au($\mathbf{L^2}_2$)]Cl.2H_2O; (c) [Au($\mathbf{L^3}_2$)]Cl.H_2O.

Table 4. UV–visible absorption data of Au complexes

Compound	Solvent	Electronic absorption bands (nm)
[Au($\mathbf{L^1}_2$)]Cl.3EtOH	MeOH	244, 282, 392
	CH_2Cl_2	241, 282
[Au($\mathbf{L^2}_2$)]Cl.2H_2O	MeOH	248, 262
	CH_2Cl_2	242, 262
[Au($\mathbf{L^3}_2$)]Cl.H_2O	MeOH	258, 325
	CH_2C_{l2}	245

to produce a filled orbital band, while overlap of the empty gold 6p orbitals produces a corresponding band of unoccupied orbitals. The excitation of an electron from the filled 5d band to the empty 6p band strengthens the bonding along these chains by removing what is effectively an antibonding electron from the 5d band and transferring that electron to the bond 6p band. The emission results from the reverse process transfer of an excited electron from the 6p band back to the 5d band. In addition, luminescence of the complexes has been attributed to self-association of the cation through aurophilic interactions, involving a pair of such d^{10} complexes to form a fully occupied set of $\sigma(d_z^2)$ and $\sigma^*(d_z^2)$ molecular orbitals involving the interaction of the filled d_z^2 orbitals, Generally, in the gold(I) complexes, it is observed that $C_{(imidazole)} \leftarrow M$ (M–L) back bonding character,

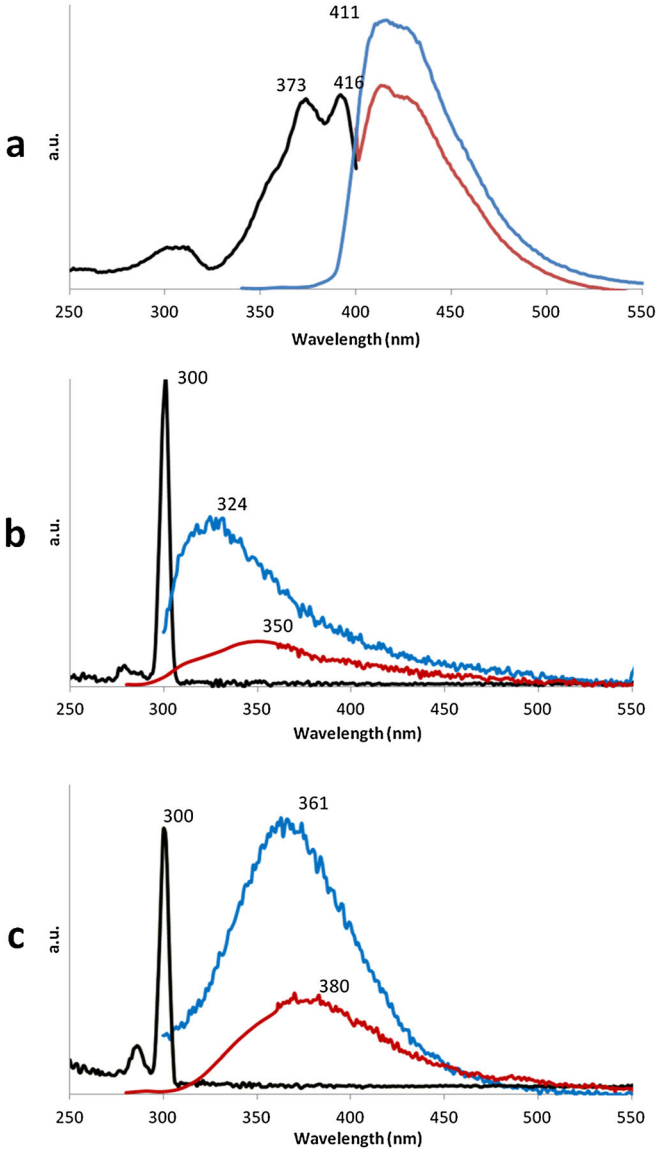

Figure 6. Excitation/emission spectra (black: excitation; red: emission at 20 °C; blue: emission at 2 °C) for Au complexes: (a) [Au($\mathbf{L^1}_2$)]Cl.3EtOH; (b) [Au($\mathbf{L^2}_2$)]Cl.2H_2O; (c) [Au($\mathbf{L^3}_2$)]Cl.H_2O.

ascribed to the greater relativistic effect of gold resulting from contraction of s and p orbitals, while the d and f orbitals remain diffuse. Specifically, the $C_{carb} \rightarrow M$ donation occurs at multiple MOs of gold(I) complexes ($\mathbf{L^1}$, $\mathbf{L^2}$ and $\mathbf{L^3}$), thus a larger L–M interaction is expected, i.e. there is interaction of the carbine lone pair of the NHC ligand fragment with the unfilled s orbital of the metal ion. Furthermore, in the complexes, a simultaneous donation from an unfilled p orbital to a π^* anti-bonding orbital of the ligand takes place. Since the ligand L has σ-donor orbitals localized on N and π-donor and π^*-acceptor orbitals delocalized on imidazole rings, the back-donation between the ligand and the Au(I) orbitals is significant. The strongest absorption in the UV region can be assigned as an intraligand π–π^* transition.

DNA Binding Studies

Among the non-platinum-based antitumor agents, gold complexes have recently gained attention because of their strong

Table 5. Fluorescence data of Au complexes

Compound	Fluorescence, λ_{max} (nm), 2 °C		Fluorescence, λ_{max} (nm), 2 °C	
	Excitation	Emission	Excitation	Emission
[Au($\mathbf{L^1}_2$)]Cl.3EtOH	373	430	390	428
[Au($\mathbf{L^2}_2$)]Cl.2H_2O	300	324	300	350
[Au($\mathbf{L^3}_2$)]Cl.H_2O	300	361	300	370

antiproliferative effects.[20,22,54–57] The successful use of auranofin (triethylphosphinegold(I) tetraacetyl thioglucose) in oral administration for the treatment of rheumatoid arthritis has gained much attention;[10,58] furthermore, auranofin and its chloro analogue Et_3PAuCl exhibit their antitumor activities due to inhibition of the enzyme thioredoxin reductase (TrxR);[54,59] in particular, auranofin has been tested for anticancer activity in *in vivo* studies of P388 leukemia in mice.[16] This means that both gold(I or III) compounds exhibit outstanding cytotoxic properties;[60–62] for example, $Au(Phen)Cl_2]PF_6$, [Au(DPQ) $Cl_2]PF_6$, $[Au(DPPZ)Cl_2]PF_6$ and $[Au(DPQC)Cl_2]PF_6$ (Phen = 1,10-phenanthroline, DPQ = dipyrido[3,2- d:2′,3′-f]quinoxaline, DPPZ = dipyrido[3,2-a:2′,3′-c] phenazine, DPQC = dipyrido[3,2-*d*:2′,3′-f]cyclohexyl quinoxaline) exhibited anticancer activity in both cisplatin-sensitive and cisplatin-resistant ovarian cancer cells.[63,64] In previous studies, it was shown that the phosphine ligand is more important for biological potency than halide or thioglucose because exchange of the carbohydrate ligand of auranofin (or the chlorine ligand of Et_3PAuCl) does not lead to a loss of antitumor activity.[18,45,55,59] Therefore, there is considerable interest in *N*-heterocyclic carbenes (NHCs) as alternatives to phosphines as ligands for the soft gold(I) ion. The relative ease of systematic modification of the NHC substituents and the comparable donor properties of NHCs to phosphines render NHCs attractive ligands.

In the present work, DNA extracted from the U373-GB cell line derived from human astrocytoma grade III (ATCC) was used for binding studies with Au complexes. The U373-GB cell line was cultured with Au complexes as described elsewhere.[40,41] We observed that the DNA was fragmented after treatment with Au complexes (Fig. 7). As shown in Fig. 7, the results reveal that in contrast to the control (lane 1) Au complexes (lanes 2–13) induced different degrees of DNA fragmentation, showing that the complexes trigger DNA fragmentation ([Au($\mathbf{L^1}_2$)]Cl.3EtOH and [Au($\mathbf{L^2}_2$)]Cl.2H_2O (10–100 μ M) but not degraded DNA (lanes 2–9); meanwhile, after treatment with [Au($\mathbf{L^3}_2$)]Cl.H_2O, both DNA fragmentation and degradation (lanes 10–13) were noted; this is probably because the presence of the benzyl ring at C3–C4 of the imidazolium ring, i.e. the substitution at C3 and C4 of the imidazolium ring could facilitate DNA degradation due to its higher DNA affinity than the *N*-imidazole-substituted compounds; this observation is consistent with reported studies.[45] At a concentration of 500 nM, [Au($\mathbf{L^3}_2$)]Cl.H_2O induced DNA fragmentation (lane 10); but at 10 μM both fragmentation and degradation were clearly observed (lanes 11–13); especially in lane 13, where complete degradation of DNA was observed. Besides, DNA fragmentation and degradation increased when the concentration of the complexes was augmented. We also observed an increase in band intensity that could be related to DNA aggregation produced by the complexes as the result of its binding with DNA.

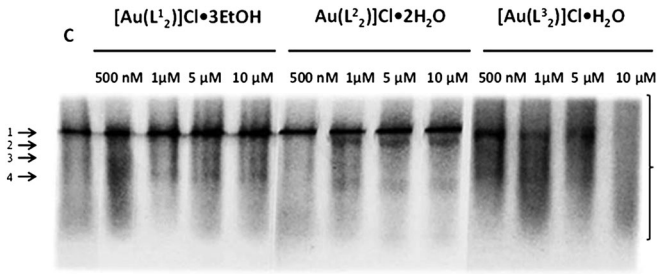

Figure 7. Effects of Au complexes on DNA aggregation, fragmentation and degradation. U373-GB cell line was treated or not (10% DMSO in water was used as vehicle) with Au complexes at different concentrations. DNA was isolated and 1 μg was separated and analyzed on 1% agarose gel and stained with gel red. The image was captured under a UV transilluminator. Arrow 1 indicates DNA free and arrows 2–4 indicate fragmented DNA. The bracket indicates degraded DNA.

Conclusion

Gold(I) complexes of 1,3-bis-pyridylimidazolium chloride ($\mathbf{L^1}$), 1,3-bis-[2,6-diisopropylphenyl]imidazolium chloride ($\mathbf{L^2}$) and 1,3-bis-[benzyl]benzimidazolium chloride ($\mathbf{L^3}$) were prepared and their spectral properties studied. A considerable intense emission band was observed for the compounds due to strong aurophilic interactions; for example, for $[Au\mathbf{L^1}_2]^+$ excitation at 373 nm, an intense emission band was observed at 430 nm in the visible region. The intensity of the emission was further increased when the temperature of the compound solution was decreased because of the increasing aurophilic interactions at the low temperature. Furthermore, the binding nature of the gold complexes with DNA isolated from the U373-GB cell line shows that the complexes, particularly [Au($\mathbf{L^3}_2$)]Cl.H_2O, fragment and degrade genomic DNA at high concentrations. Furthermore, the intensities of the fragmented bands increased when the concentration of the metal complex augmented; this increase in band intensity could be related to DNA aggregation produced by the Au complex as the result of its DNA binding.

Supporting information

Supporting information may be found in the online version of this article.

Acknowledgments

The authors acknowledge Direccíon General de Asuntos del Personal Académico (Project PAPIIT No. IN226310) for economic support and the bilateral project Consejo Nacional Ciencia y Tecnología (CONACYT), Department of Science and Technology (DST), for travel expenses to India. The authors also thank DGSCA-UNAM for computation facilities.

References

[1] A. V. Klein, T. W. Hambley, *Chem. Rev.* **2009**, *109*, 4911.
[2] O. Rixe, W. Ortuzar, M. Alvarez, R. Parker, E. Reed, K. Paull, T. Fojo, *Biochem. Pharmacol.* **1996**, *52*, 1855.
[3] B. Spingler, D. A. Whittington, S. J. Lippard, *Inorg. Chem.* **2001**, *40*, 5596.
[4] M. Galanski, M. A. Jakupec, B. K. Keppler, *Curr. Med. Chem.* **2005**, *12*, 2075.
[5] E. Wong, C. M. Giandomenico, *Chem. Rev.* **1999**, *99*, 2451.
[6] J. Reedijk, *Chem. Rev.* **1999**, *99*, 2499.
[7] I. Ot, R. Gust, *Arch. Pharm.* **2007**, *340*, 117.
[8] L. Ronconi, P. J. Sadler, *Coord. Chem. Rev.* **2007**, *251*, 1633.
[9] P. C. A. Bruijnincx, P. J. Sadler, *Curr. Opin. Chem. Biol.* **2008**, *12*, 197.
[10] I. Ott, *Coord. Chem. Rev.* **2009**, *253*, 1670.
[11] E. A. Pacheco, E. R. T. Tiekink, M. W. Whitehouse, Gold Chemistry: Applications and Future Directions in the Life Sciences, Wiley, Chichester, **2009**.
[12] S. Y. Ho, E. R. T. Tiekink, Metallotherapeutic Drugs and Metalbased Agents: The Use ofMetals in Medicine, Wiley, Chichester, **2005**.
[13] S. Josch, C. Wetzel, P. Boehler, S. Havermann, M. Schmuck, K. Dach, P. C. Kunz, W. Waetjen, *Naunyn Schmiedebergs Arch. Pharmacol.* **2011**, *383*, 100.
[14] S. Lisowsky, S. Josch, S. Havermann, G. Fritz, P. C. Kunz, C. Wetzel, W. Waetjen, *Naunyn Schmiedebergs Arch. Pharmacol.* **2012**, *385*, 53.
[15] A. Nakhla, D. Ackermann, S. Havermann, P. C. Kunz, M. Braun, G. Fritz, W. Waetjen, *Naunyn Schmiedebergs Arch. Pharmacol.* **2012**, *385*, 62.
[16] V. Gandin, A. P. Fernandes, M. P. Rigobello, B. Dani, F. Sorrentino, F. Tisato, M. Bjornstedt, A. Bindoli, A. Sturaro, R. Rella, C. Marzano, *Biochem. Pharmacol.* **2010**, *79*, 90.
[17] S. J. Berners-Price, C. K. Mirabelli, R. K. Johnson, M. R. Mattern, F. L. McCabe, L. F. Faucette, C. M. Sung, S. M. Mong, P. J. Sadler, S. T. Crooke, *Cancer Res.* **1986**, *46*, 5486.
[18] C. K. Mirabelli, R. K. Johnson, D. T. Hill, L. F. Faucette, G. R. Girard, G. Y. Kuo, C. M. Sung, S. T. Crooke, *J. Med. Chem.* **1986**, *29*, 218.
[19] C. Wetzel, P. C. Kunz, M. U. Kassack, A. Hamacher, P. Boehler, W. Watjen, I. Ott, R. Rubbiani, B. Spingler, *Dalton Trans.* **2011**, *40*, 9212.
[20] P. J. Barnard, S. J. Berners-Price, *Coord. Chem. Rev.* **2007**, *251*, 1889.
[21] P. J. Barnard, M. V. Baker, S. J. Berners-Price, B. W. Skelton, A. H. White, *Dalton Trans.* **2004**, 1038.
[22] S. J. Berners-Price, A. Filipovska, *Aust. J. Chem.* **2008**, *61*, 661.
[23] G. D. Hoke, R. A. Macia, P. C. Meunier, P. J. Bugelski, C. K. Mirabelli, G. F. Rush, W. D. Matthews, *Toxicol. Appl. Pharmacol.* **1989**, *100*, 293.
[24] G. D. Hoke, G. F. Rush, G. E. Bossard, J. V. McArdle, B. D. Jensen, C. K. Mirabelli, *J. Biol. Chem.* **1988**, *263*, 11203.
[25] M. J. Frisch, G. W. Trucks, H. B. Schlegel, G. E. Scuseria, M. A. Robb, J. R. Cheeseman, J. A. Montgomery Jr., T. Vreven, K. N. Kudin, J. C. Burant, J. M. Millam, S. S. Iyengar, J. Tomasi, V. Barone, B. Mennucci, M. Cossi, G. Scalmani, N. Rega, G. A. Petersson, H. Nakatsuji, M. Hada, M. Ehara, K. Toyota, R. Fukuda, J. Hasegawa, M. Ishida, T. Nakajima, Y. Honda, O. Kitao, H. Nakai, M. Klene, X. Li, J. E. Knox, H. P. Hratchian, J. B. Cross, C. Adamo, J. Jaramillo, R. Gomperts, R. E. Stratmann, O. Yazyev, A. J. Austin, R. Cammi, C. Pomelli, J. W. Ochterski, P. Y. Ayala, K. Morokuma, G. A. Voth, P. Salvador, J. J. Dannenberg, V. G. Zakrzewski, S. Dapprich, A. D. Daniels, M. C. Strain, O. Farkas, D. K. Malick, A. D. Rabuck, K. Raghavachari, J. B. Foresman, J. V. Ortiz, Q. Cui, A. G. Baboul, S. Clifford, J. Cioslowski, B. B. Stefanov, G. Liu, A. Liashenko, P. Piskorz, I. Komaromi, R. L. Martin, D. J. Fox, T. Keith, M. A. Al-Laham, A. N. C. Y. Peng, M. Challacombe, P. M. W. Gill, B. Johnson, W. Chen, M. W. Wong, C. Gonzalez, J. A. Pople, Gaussian, revision D 01 edn, Gaussian, Wallingford, CT, **2004**.
[26] A. D. Becke, *Phys. Rev. A* **1988**, *38*, 3098.
[27] C. T. Lee, W. T. Yang, R. G. Parr, *Phys. Rev. B* **1988**, *37*, 785.
[28] P. J. Hay, W. R. Wadt, *J. Chem. Phys.* **1985**, *82*, 299.
[29] V. J. Catalano, A. O. Etogo, *Inorg. Chem.* **2007**, *46*, 5608.
[30] P. de Fremont, N. M. Scott, E. D. Stevens, S. P. Nolan, *Organometallics* **2005**, *24*, 2411.
[31] P. de Fremont, N. M. Scott, E. D. Stevens, T. Ramnial, O. C. Lightbody, C. L. B. Macdonald, J. A. C. Clyburne, C. D. Abernethy, S. P. Nolan, *Organometallics* **2005**, *24*, 6301.
[32] A. J. Arduengo, R. Krafczyk, R. Schmutzler, H. A. Craig, J. R. Goerlich, W. J. Marshall, M. Unverzagt, *Tetrahedron* **1999**, *55*, 14523.
[33] N. Kuhn, T. Kratz, *Synthesis – Stuttgart* **1993**, 561.
[34] L. Ray, M. M. Shaikh, P. Ghosh, *Dalton Trans.* **2007**, 4546.
[35] M. J. Ping, *Adv. Mater. Res.* **2012**, *554–556*, 1686.
[36] R. Uson, A. Laguna, M. Laguna, D. A. Briggs, H. H. Murray, J. P. Fackler, *Inorg. Synth.* **1989**, *26*, 85.
[37] P. C. Kunz, M. U. Kassack, A. Hamacher, B. Spingler, *Dalton Trans.* **2009**, 7741.
[38] V. J. Catalano, M. A. Malwitz, A. O. Etogo, *Inorg. Chem.* **2004**, *43*, 5714.
[39] D. Rios, M. M. Olmstead, A. L. Balch, *Inorg. Chem.* **2009**, *48*, 5279.
[40] G. Gonzalez-Agueero, A. A. Gutierrez, D. Gonzalez-Espinosa, J. D. Solano, R. Morales, A. Gonzalez-Arenas, E. Cabrera-Munoz, I. Camacho-Arroyo, *Endocrine* **2007**, *32*, 129.
[41] E. Cabrera-Munoz, A. Gonzalez-Arenas, M. Saqui-Salces, J. Camacho, F. Larrea, R. Garcia-Becerra, I. Camacho-Arroyo, *J. Steroid Biochem. Mol. Biol.* **2009**, *113*, 80.
[42] R. G. Pearson, *Inorg. Chim. Acta* **1998**, *270*, 252.
[43] R. G. Pearson, *J. Chem. Ed.* **1999**, *76*, 267.
[44] D. Mishra, A. Barbieri, C. Sabatini, M. G. B. Drew, H. M. Figgle, W. S. Sheldrick, S. K. Chattopadhyay, *Inorg. Chim. Acta* **2007**, *360*, 2231.
[45] W. Liu, K. Bensdorf, M. Proetto, U. Abram, A. Hagenbach, R. Gust, *J. Med. Chem.* **2011**, *54*, 8605.
[46] H.-h. Gao, C.-h. Yan, X.-P. Tao, Y. Xia, H.-M. Sun, Q. Shen, Y. Zhang, *Organometallics* **2010**, *29*, 4189.
[47] R. J. Baker, A. J. Davies, C. Jones, M. Kloth, *J. Organomet. Chem.* **2002**, *656*, 203.
[48] R. J. Baker, H. Bettentrup, C. Jones, *Eur. J. Inorg. Chem.* **2003**, 2446.
[49] E. D. Blue, T. B. Gunnoe, J. L. Petersen, P. D. Boyle, *J. Organomet. Chem.* **2006**, *691*, 5988.
[50] A. Sidiropoulos, C. Jones, A. Stasch, S. Klein, G. Frenking, *Angew. Chem. Int. Ed.* **2009**, *48*, 9701.
[51] S. K. Chastain, W. R. Mason, *Inorg. Chem.* **1982**, *21*, 3717.
[52] R. L. White-Morris, M. Stender, D. S. Tinti, A. L. Balch, D. Rios, S. Attar, *Inorg. Chem.* **2003**, *42*, 3237.
[53] T. E. Muller, S. W. K. Choi, D. M. P. Mingos, D. Murphy, D. J. Williams, V. W. W. Yam, *J. Organomet. Chem.* **1994**, *484*, 209.
[54] G. Gasser, I. Ott, N. Metzler-Nolte, *J. Med. Chem.* **2011**, *54*, 3.
[55] S. J. Berners-Price, A. Filipovska, *Metallomics* **2011**, *3*, 863.
[56] S. Nobili, E. Mini, I. Landini, C. Gabbiani, A. Casini, L. Messori, *Med. Res. Rev.* **2010**, *30*, 550.
[57] A. Bindoli, M. P. Rigobello, G. Scutari, C. Gabbiani, A. Casini, L. Messori, *Coord. Chem. Rev.* **2009**, *253*, 1692.
[58] K. C. Dash, H. Schmidbauer, Metal Ions in Biological Systems, Marcel Dekker, New York, **1982**.
[59] I. Ott, X. Qian, Y. Xu, D. H. W. Vlecken, I. J. Marques, D. Kubutat, J. Will, W. S. Sheldrick, P. Jesse, A. Prokop, C. P. Bagowski, *J. Med. Chem.* **2009**, *52*, 763.
[60] M. A. Calvo-Garcia, B. M. Kline-Fath, M. A. Levitt, F.-Y. Lim, L. E. Linam, M. N. Patel, S. Kraus, T. M. Crombleholme, A. Pena, *Pediatr. Radiol.* **2011**, *41*, 1117.
[61] J. A. Lessa, J. C. Guerra, L. F. de Miranda, C. F. D. Romeiro, J. G. Da Silva, I. C. Mendes, N. L. Speziali, E. M. Souza-Fagundes, H. Beraldo, *J. Inorg. Biochem.* **2011**, *105*, 1729.
[62] M. Arsenijevic, M. Milovanovic, V. Volarevic, A. Djekovic, T. Kanjevac, N. Arsenijevic, S. Dukic, Z. D. Bugarcic, *Med. Chem.* **2012**, *8*, 2.
[63] K. Palanichamy, N. Sreejayan, A. C. Ontko, *J. Inorg. Biochem.* **2012**, *106*, 32.
[64] K. Palanichamy, A. C. Ontko, *Inorg. Chim. Acta* **2006**, *359*, 44.